8-13-2019

GABAergic Inhibition of Brainstem Neurons Involved in Breathing Regulation is Disrupted in Rett Syndrome

Colin Arrowood

GABAERGIC INHIBITION OF BRAINSTEM NEURONS INVOLVED IN BREATHING REGULATION IS DISRUPTED IN RETT SYNDROME

by

COLIN ARROWOOD

Under the Direction of Chun Jiang, PhD

ABSTRACT

GABA is the prominent inhibitory neurotransmitter in the brain and defects in the GABA system are attributable to several genetic diseases including Rett Syndrome (RTT). People with RTT show characteristic breathing disorders, suggesting a link with defects in the GABA system. Noradrenergic neurons in the locus coeruleus (LC) are CO_2 chemosensitive and play a role in breathing regulation. We conducted experiments to find out if activation of a novel group of dorsomedial LC GABAergic neurons causes instantaneous firing rate changes in LC neurons. Spike train recordings with cross-correlation analysis suggests that the dmLC neurons made monosynaptic and oligosynaptic connections with the LC neurons. The GABAergic inhibition appeared to have major effects on medullary respiratory neurons, as our results showed that THIP, the extrasynaptic GABA receptor agonist, suppressed excitations in these cells. The

results from these experiments provide new evidence for the GABAergic inhibition of brainstem neurons involved in breathing control.

INDEX WORDS: Locus coeruleus, Optogenetics, Rett Syndrome, MEA, Microelectrode Array, Transgenic, In-vitro

GABAERGIC INHIBITION OF BRAINSTEM NEURONS INVOLVED IN BREATHING REGULATION IS DISRUPTED IN RETT SYNDROME

by

COLIN ARROWOOD

A Thesis Submitted in Partial Fulfillment of the Requirements for the Degree of

Master of Science

in the College of Arts and Sciences

Georgia State University

2019

GABAERGIC INHIBITION OF BRAINSTEM NEURONS INVOLVED IN BREATHING REGULATION IS DISRUPTED IN RETT SYNDROME

by

COLIN ARROWOOD

Committee Chair: Chun Jiang

Committee: Vincent Rehder

Kyle Frantz

Electronic Version Approved:

Office of Graduate Studies

College of Arts and Sciences

Georgia State University

July 2019

DEDICATION

I would like to dedicate this thesis to my loving friends and family who have supported and encouraged me.

To the love of my life, Erin Gallagher, who stood by my side with boundless love the whole way.

ACKNOWLEDGEMENTS

I would like to acknowledge the members of my committee who truly represent the excellence of the Georgia State University Biology Masters program: My advisor, Chun Jiang, Ph.D., Kyle Frantz, Ph.D., and Vincent Rehder, Ph.D. I'm truly fortunate to have had their thoughtful consideration and expertise in designing these experiments, and their guidance and exacting critique of this written document. I'm particular thankful for the help Ningren Cui, Ph.D., provided me in facilitating and aiding the experimentation process.

The Jiang Lab has been a guiding hand during my time here at Georgia State University, and the student scientists in this lab have always been helpful and friendly. I couldn't have found a better place to learn how to conduct research.

I would also like to specifically thank Yang Wu , who conducted the *in vivo* electrophysiology and plethysmography experiments outlined in Sub Aim 2, and for allowing me to aid in the data analysis of this research. The results of this study went into the following publication:

Wu, Y., Cui, N., Xing, H., Zhong, W., Arrowood, C., Johnson, C. M., & Jiang, C. (2019). Mecp2 Disruption in Rats Causes Reshaping in Firing Activity and Patterns of Brainstem Respiratory Neurons. *Neuroscience*, *397*, 107–115. doi:10.1016/j.neuroscience.2018.11.011

TABLE OF CONTENTS

LIST OF FIGURES

1 INTRODUCTION

The mammalian brainstem contains a nucleus that is a primary center of norepinephrine (NE), this region is called the locus coeruleus (LC). The majority of noradrenergic neurons in mammalian CNS are located in this brain region. [1] As such, the LC is critical for many physiological functions and behaviors ranging from motor function and breathing activity to anxiety and psychosis. [2] The neurons in this region project through axonal networks to the forebrain, cerebellum, and the medulla, and project to these regions in a non-homogenous way. [2], [3] The specific cellular mechanisms behind these pathways and the physical location of these networks could be better understood by investigating the electrophysiology taking place. It has been shown that alterations in the firing rate and of LC neurons has been correlated to a diverse group of behavioral responses. [4] Recently it has been suggested that neurotransmitter release varies in intensity from the LC to other regions of the brainstem. It has been thought this occurs throughout the CNS and denotes distinct pathways that the LC may be use. [5] The compilation of these findings suggests there are routes for LC input to and from a multitude of networks, but indicates there is yet more to be done to specifically identify and characterize this region. [6], [7]

The dorsomedial GABAergic nucleus near the LC has been discovered to cause direct inhibition of noradrenergic LC neurons. [8] An optogenetic approach was utilized to demonstrate these phenomena, and inhibition of noradrenergic LC neurons was observed after light activation of GABAergic neurons in this nucleus.[8] Optogenetics is a novel electrophysiological technique which relies on the insertion of specific genes to express light sensitive ion channels in the plasma membrane. [1], [8] Optogenetics was also employed to identify the link between the firing rate of noradrenergic LC neurons and different behaviors, which indicated that firing rate is associated with the activation of various pathways. [1] Unfortunately, despite combining this

optogenetic approach with the dual patch clamp technique, direct evidence for these phenomena remained elusive.

We propose the use of microelectrode arrays (MEA) as an alternative to the patch clamp technique. MEA's have the advantage of higher throughput by recording numerous electrogenic cells at one time across a large region of tissue. Using the optogenetic approach developed in the previous study,[8] and coupled with an extensive number of recording electrodes, the opportunity to capture the synaptic communication occurring between these two cellular clusters should improve substantiality. We could then use auto and cross-correlation analysis to reference the GABAergic signal and visualize the immediate inhibitory effect of the GABAergic neurons. Finding evidence of this inhibitory effect happening in the same layer of the brainstem that was investigated previously would provide support for the hypothesis that this nucleus is in fact directly acting on the noradrenergic LC neurons, and in turn would help to shed light on the neural pathways at play in this important region of the CNS.

Understanding how the interactions of GABAergic neurons on LC neurons is critical to investigating how the brainstem region is disrupted in patients with Rett Syndrome (RTT). Mouse and rat models of the disease have been created by knocking of the gene *Mecp2*, which has been associated with RTT. [9], [10] Research conducted on these mouse models have found that there is an imbalance in the excitation and inhibition in the CNS correlating with the disease. The disruption in excitation/inhibition is found in many brain regions, including that of the hippocampus and the brainstem. [11], [10] Neurons in the LC were found to be excessively excitatory, and this was subsequently attributed to reduced GABAergic inhibition and defects in the intrinsic membrane properties. [10], [12] Investigating the disruption of GABAergic input in this disease state can illuminate the ways that these neurons interact with other regions in the

brainstem. Inducing Mecp2 knockout in rats allows for access of the brainstem using a direct *in vivo* microelectrode approach with the animal. Accessing the phrenic nerve, we can study and characterize the electrophysiology of the breathing pattern as a series of field potentials. Once characterized, the knockout model can be utilized to investigate how GABAergic inputs can be rectified using drug treatments and how those treatments affect different brainstem regions. The type of effect GABA agonist (THIP) and reuptake blockers (NNC-711), have in a disrupted disease state, could allow us to understand the how the LC is also controlled by nearby GABAergic inputs.

1.1 **Review of Literature**

1.1.1 The Locus Coeruleus

The Wenzel brothers named the locus coeruleus (LC) in 1812 for its blue-black color. [13] The LC is a dorsal pontine nucleus located near the pontomesencephalic junction and the floor of the fourth ventricle.[13] Inside this nucleus reside a dense cluster of norepinephrine (NE) producing neurons which create the most significant collection of neurons producing NE in the central nervous system. [13] Through branching efferent projections, the LC provides input for several areas of the brain and the spinal cord. [14]

Similarly to the array of LC efferent projections, the inputs are also very heterogeneous, an observation that displays the complex nature and varied functionality of this modulatory neural nucleus. [15], [16] It has been demonstrated that the LC is involved with a multitude of responses, ranging from attention, arousal and memory, to stress, panic, fear and respiratory control.[17] The physiology and neuroanatomy of this cluster of neurons truly demonstrate the significance of its role in the control and integration of these autonomic systems.

1.1.2 GABAergic Input to the Locus Coeruleus

It's well known that LC neuronal activity is inhibited by y-aminobutyric acid (GABA) afferents. Alterations in the physiological or pathological conditions influencing these GABAergic inputs can cause specific LC neuronal firing patterns. Increases in GABA release has been found to have an effect in lowering the firing frequency of LC neurons during REM sleep, and the effect was mitigated when antagonists for $GABA_A$ receptors were administered. Rett Syndrome is a disease where there are significant defects in pre- and post-synaptic GABAergic systems which correlate with hyper-excitability in LC neurons. [12], [18]

Prior research has found that there are a number of areas in the brain contributing to GABAergic input of the LC, including the forebrain and medullary nuclei. Neuronal networks in the nearby local area have only recently been demonstrated and had previously been quite elusive, particularly GABAergic inhibition.[8] It still is not clear what intrinsic properties the GABAergic neurons have, whether they form an isolated group or how they interact with the LC region. A major hurdle in studying these local GABAergic neurons is that it is difficult to identify these specific cell-types in communication through electrophysiology.

1.1.3 GABAergic Disruption in Rett Syndrome

Rett Syndrome is a neurodevelopmental disease caused by mutations in the gene MECP2. People who suffer from this disorder have autonomic dysfunctions, and these dysfunctions often lead to sudden death. The majority of patients with this syndrome suffer from abnormalities in their breathing which can be characterized as episodic hyper- and hypoventilation. When Mecp2 disruption is reproduced in animal models, these breathing abnormalities can be similarly identified. Neurons located in the LC are identified to be excessively excitable in *Mecp2* knockout mice.[10] The hyperexcitability is associated with the GABA system as *Mecp2* gene

disruption causes Rett Syndrome associated characteristics, such as decreased activiation in GABAergic neurons. [19] The breathing abnormalities caused by the Rett Syndrome and *Mecp2* knockout form a functional disease model to illuminate the inhibitory interactions between the LC and nearby GABAergic neurons.

1.1.4 The Advantages of Microelectrode Arrays

The microelectrode array (MEA) technique, when compared to traditional electrophysiology, is more advantageous any many respects in that it enables: the evaluation of spatiotemporal arrangements of network-level electrical activity; the acquisition of huge amounts of spatial information on network dynamics using multisite recordings; the analysis of network physiological characteristics and the pharmacological effects of drugs. [20], [21], [22] The MEA is particularly well suited for studying rhythmic activity, pharmacological drug testing, synaptic plasticity, and single-unit activity.[23], [24], [25], [26] Additionally, the data recorded from these devices can be analyzed using powerful software tools that allow for broad sets of analysis for various applications.

1.2 **Hypothesis**

Noradrenergic neurons involved with breathing regulation in the locus coeruleus can be inhibited through GABAergic inputs that are disrupted in Rett Syndrome.

Specific Aim 1: Does activation and inhibition of GABAergic neurons in the dorsomedial region of the locus coeruleus produce instantaneous changes in firing activity of noradrenergic neurons in the LC?

- *Sub-Aim 1*: Can the opto-activation of GABAergic neurons in the dorsomedial region of the LC produce monosynaptic inhibition of noradrenergic LC neurons?

- *Sub-Aim 2*: Does GABAergic activation through chemical agonists or re-uptake inhibitors produce inhibition in regions of the brainstem where neurons are involved with breathing regulation?

2 MATERIALS AND METHODS – SUB AIM 1

2.1 Transgenic animals

All animal procedures were carried out following the guidelines of the National Institutes of Health (NIH) *Guide for the Care and Use of Laboratory Animals*, and were agreed upon by the Georgia State University Institutional Animal Care and Use Committee. Cross-breeding was utilized to create the transgenic mice by breeding a strain of GAD2-Cre mice (Gad2tm2(cre)Zjh/J, Jackson Laboratory SN 010802) with a ChR2-eYFP-LoxP strain (B6;129S-Gt(ROSA) 26Sortm32(CAG-COP4H134R/EYFP)Hze/J, Jackson Laboratory SN 12569). Offspring from this cross-breeding were genotyped on a regular basis with a protocol for PCR designed by the Jackson Laboratory.

2.2 Brain slice preparation

Animals between the ages of 4-8 weeks were deeply anesthetized via inhalation of saturated isoflurane and then a transcardial perfusion was performed with 15-25 mL of room temperature carbogenated N-methyl-D-glucamine artificial cerebrospinal fluid (NMDG aCSF) (NMD GaCSF: 92 mM NMDG, 2.5 mM KCl, 1.25 mM NaH2PO4, 30 mM NaHCO3, 20 mM HEPES, 25 mM glucose, 2 mM thiourea, 5 mM Na-ascorbate, 3 mM Na-pyruvate, 0.5 mM CaCl2·4H2O and 10 mM MgSO4·7H2O. Ph was titrated to 7.3–7.4 with concentrated hydrochloric acid). Animals were then decapitated, and the brainstem was sectioned from the brain and removed quickly to be placed in a room temperature NMDG aCSF solution. Traverse pontine sections (250 μM) with the LC exposed on the surface, were produced using a vibratome (Series 1000, The Vibratome Company, St. Louis, MO) in the carbogenated room temperature NMDG aCSF. The slices were collected and placed in NMDG aCSF at 32-34°C for 12 minutes to recover from the procedure. After the 12-minute incubation, the slices were transferred to a

HEPES aCSF (HEPES holding aCSF: 92 mM NaCl, 2.5 mM KCl, 1.25 mM NaH_2PO_4, 30 mM $NaHCO_3$, 20 mM HEPES, 25 mM glucose, 2 mM thiourea, 5 mM Na-ascorbate, 3 mM Na-pyruvate, 2 mM $CaCl_2 \cdot 4H_2O$ and 2 mM $MgSO_4 \cdot 7H_2O$) that was carbogenated and maintained at room temperature. Slices that were used for recording were transferred to a recording MEA that was perfused using carbogenated recording aCSF (Recording aCSF: 119 mM NaCl, 2.5 mM KCl, 1.25 mM NaH_2PO_4, 24 mM $NaHCO_3$, 12.5 mM glucose, 2 mM $CaCl_2 \cdot 4H_2O$ and 2 mM $MgSO_4 \cdot 7H_2O$) at a 10 mL/min rate and the temperature was set to 37°C.

2.3 **Optostimulation of GABAergic neurons**

GABAergic neurons with YFP expression were identified via optostimulation using a xenon light source with a high-speed switcher (Lambda GD-4, Sutter Instruments, Novato, CA). The source of the light was channeled through a fiber optic cable positioned 1-2 cm above the MEA and brain slice, and blue light was delivered through a 470 nm bandpass filter. The latency of the light-evoked action potentials was measured from the onset of the action potential when compared to the onset of the light activation.

2.4 **Electrophysiology**

The microelectrode array (MEA) recordings were conducted using brain slices with positioning done under a microscope (microscope details) at 4X resolution. The slices were delicately positioned so that the LC and dorsal LC were centered over the 64-electrode array as shown in Fig. 1. The slice was held down using a nylon mesh and anchor made of stainless steel, and submerged in recording aCSF that was carbogenated, heated to 37°C, and perfused continuously at 10 mL/min. The slices were generally recorded for >45 min, a period of time that proved sufficient for the experimental protocol. Experiments were conducted only when optostimulation of GABAergic neurons was observed. When averaging multiple recordings from

a single slice, the variability between the recording locations was taken into account to produce repeatable results between experiments.

The electrophysiological data was acquired using the Mobius software supplied by AlphaMED to record the raw signals. The data was then analyzed using Neuroexplorer 3.0 software to interpret the waveform and spike detection data taken using the Mobius software. Data is depicted as the mean ± SE.

3 RESULTS – SUB AIM 1

3.1 Optostimulation of GABAergic dmLC Neurons on a MEA

Of the 64 recording electrodes in the MEA probe, 11 were electroactive, of which 8 displayed GABAergic optoactivation and 3 displayed what appeared to be inhibition (Fig 3 Bottom). The stimulation of neurons in the dmLC by 470 nm blue light has been established to cause inhibition of firing activity in LC neurons in previous patch clamp studies. [8] Previous literature found that only a subset of dmLC neurons fired spontaneously, which could explain why only 2 of the 8 GABAergic optoactivated neurons fired spontaneously throughout the recording.[8] Optostimulation of these neurons produced action potentials at a high frequency (Fig 7)

3.2 Inhibition of LC Neurons by dmLC GABAergic Interneurons

To achieve an understanding for how the dmLC neurons interacted with the LC neurons, the response of LC neurons was investigated on the MEA following optostimulation. The dmLC nucleus is located next to the LC neurons which are densely packed near the lateral floor of the 4th ventricle in the dorsolateral pons, so the array was arranged to maximize the number of electrodes that would be exposed to these neurons (Fig 2C, 2D, and 3 Top). The neurons of the LC are well known to show tonic spontaneous firing activity that result from their intrinsic membrane properties. The electrodes that fired most tonically did not demonstrate any optoactivation following application of 470 nm blue light that flooded the MEA chamber (Fig 1, and 3 Middle). These neurons appeared to show decreased firing rates during the periods of light application, which would agree with previous studies that showed that LC neurons where inhibited during light activation (Fig 7).[8] In the same 700 micron square area there is GABAergic optoactivation where the dmLC interneurons have been found to reside next to the

LC nucleus. When light is applied to the brain slice the inter-spike interval of the LC neurons increases, while the GABAergic neurons that are inactive during this period are activated and have a much lower ISI, as associated with optoactivation of the neurons and frequent depolarization (Fig 5). The inter-spike interval is noticeably alternated during the period of light application, with inhibition of LC neurons being represented by less frequent events and increases ISI (Fig 6).

The firing activity of LC neurons was referenced to electrodes designated as GABAergic neurons to look at correlation in activity between the two different cell types (Fig 8). The cross-correlogram of the LC neurons demonstrates the formation of a valley around zero when referenced to the GABAergic neurons, a sign of a lack of depolarization in LC neurons immediately following GABAergic depolarization. The cross-correlation suggests that firing activity of the LC neurons is delayed when referenced to the GABAergic input, possibly showing an inhibitory interaction between the two cell types. The increase in firing events taking place around 1 ms from the GABAergic neuron signals demonstrates a consistent delay in the firing activity following optostimulation of the GABAergic neurons.

The results from the optostimulation experiments suggest that the LC neuronal inhibition is primarily driven monosynaptically through the dmLC optostimulation and not via axonal terminals of GABAergic or DTN neurons. There are a number of reasons to conclude this; the LC neuronal inhibition is calculated to be monosynaptic based on the direct inhibition by the dmLC as opposed to disinhibition through another neuron, the inhibition of the LC neurons is not observed in the brain slices where the dmLC is missing, and the antidromic field potentials in the DTN cannot be created from the dmLC optostimulation. However, even though these reasons can explain a possible monosynaptic relationship, it is still possible that light may activate the

axons of GABAergic cellular bodies that are in other regions or no longer remain intact in the brain slice. Discovering more direct evidence for monosynaptic inhibition of LC neurons by the dmLC cells remains warranted, as an oligosynaptic interaction could also be taking place. Further studies will have to done to pinpoint these interactions.

For instance, it is well established that truncated axons even without a soma can still generate action potentials based on the stimulation strength and the remaining axonal length. The brain slice MEA results did not show inhibition of the LC in absence of the dmLC, so they do not agree with a process of LC neuronal inhibition by means of truncated axons, but this explanation cannot be completely disproven either. It is then suggested that there is synaptic inhibition of the LC neurons by the dmLC, but it cannot be conclusively confirmed. Evidence should be obtained by means outside the approach of optogenetics to prove this interaction, that is of course outside the limits of this study. Further studies should focus on the synaptic interactions taking place

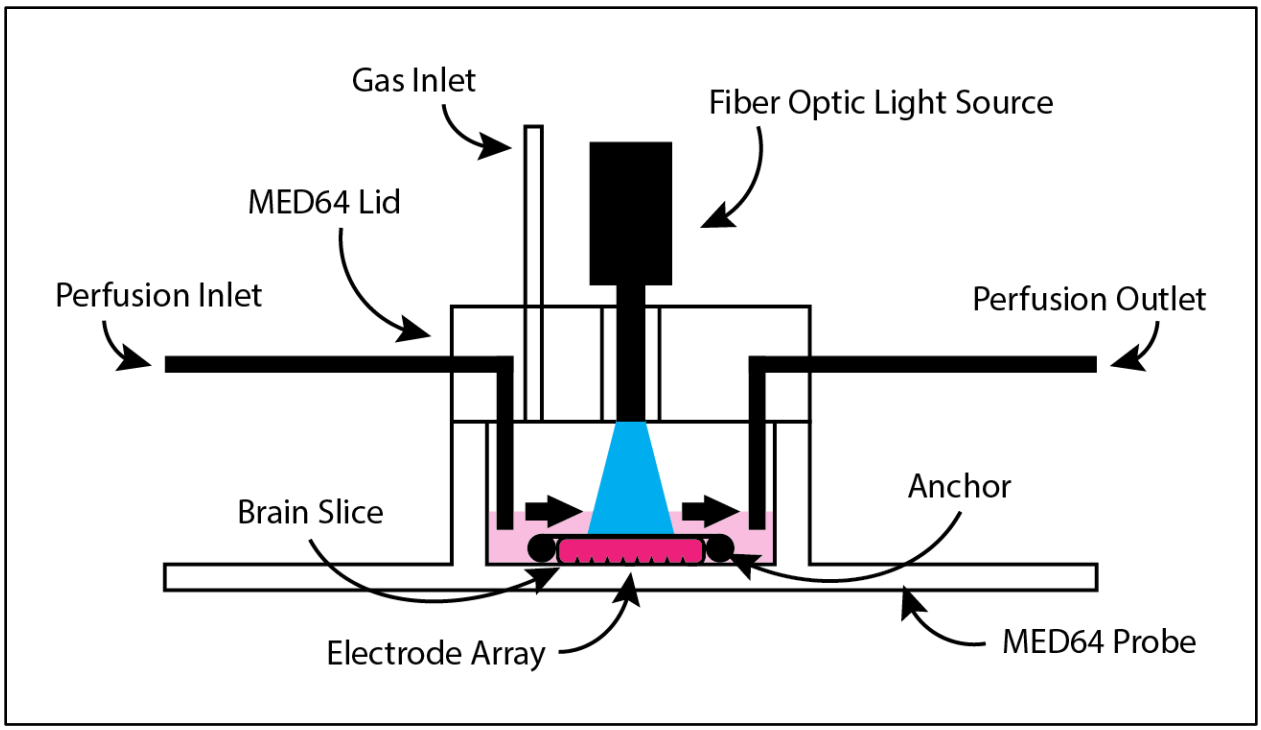

Figure 1. Side View Schematic Representation of the Microelectrode Array Experimental Setup.
The fiber optic light source is positioned 2-3 cm from the brain slice and as shown above, the light from this fiber optic cable covers the entire exposed slice. Perfusion of a carbogenated aCSF is shown to flow across the slice in one direction and transported out using a peristaltic pump system.

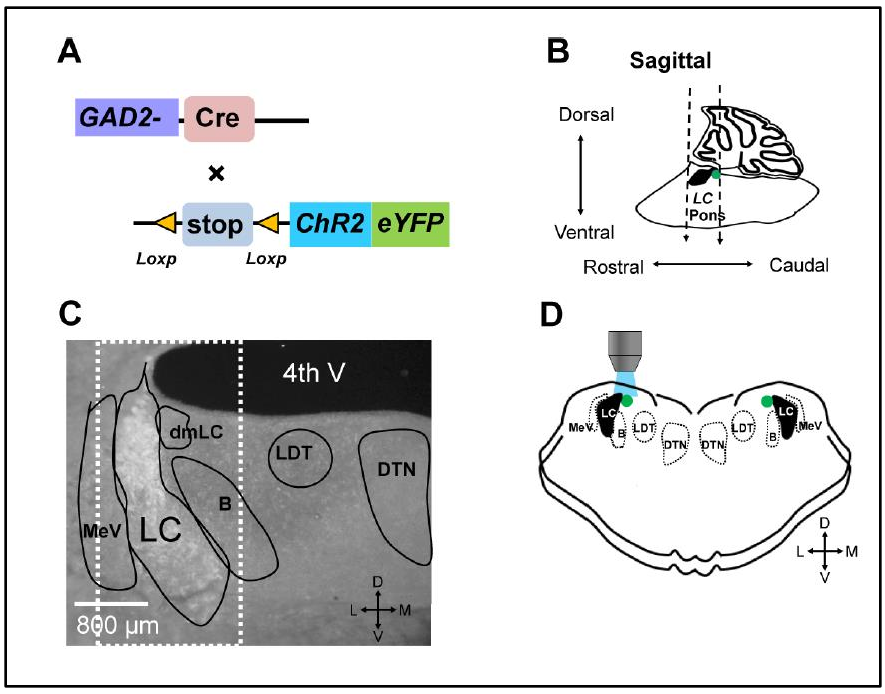

Figure 2. Overview of Transgenic Expression of Optogenetic Channels and the Location of the dmLC Neurons in a Brainstem Slice

A) The strategy for the transgenic expression of ChR2 (H134R) in GABAergic neurons. (B) A view of the brain region used in this study shown from the sagittal perspective, the dmLC region in green. (C) The typical large LC neurons are framed in the white.[8] (D) Diagram showing the position of the dmLC in a brainstem slice (green).

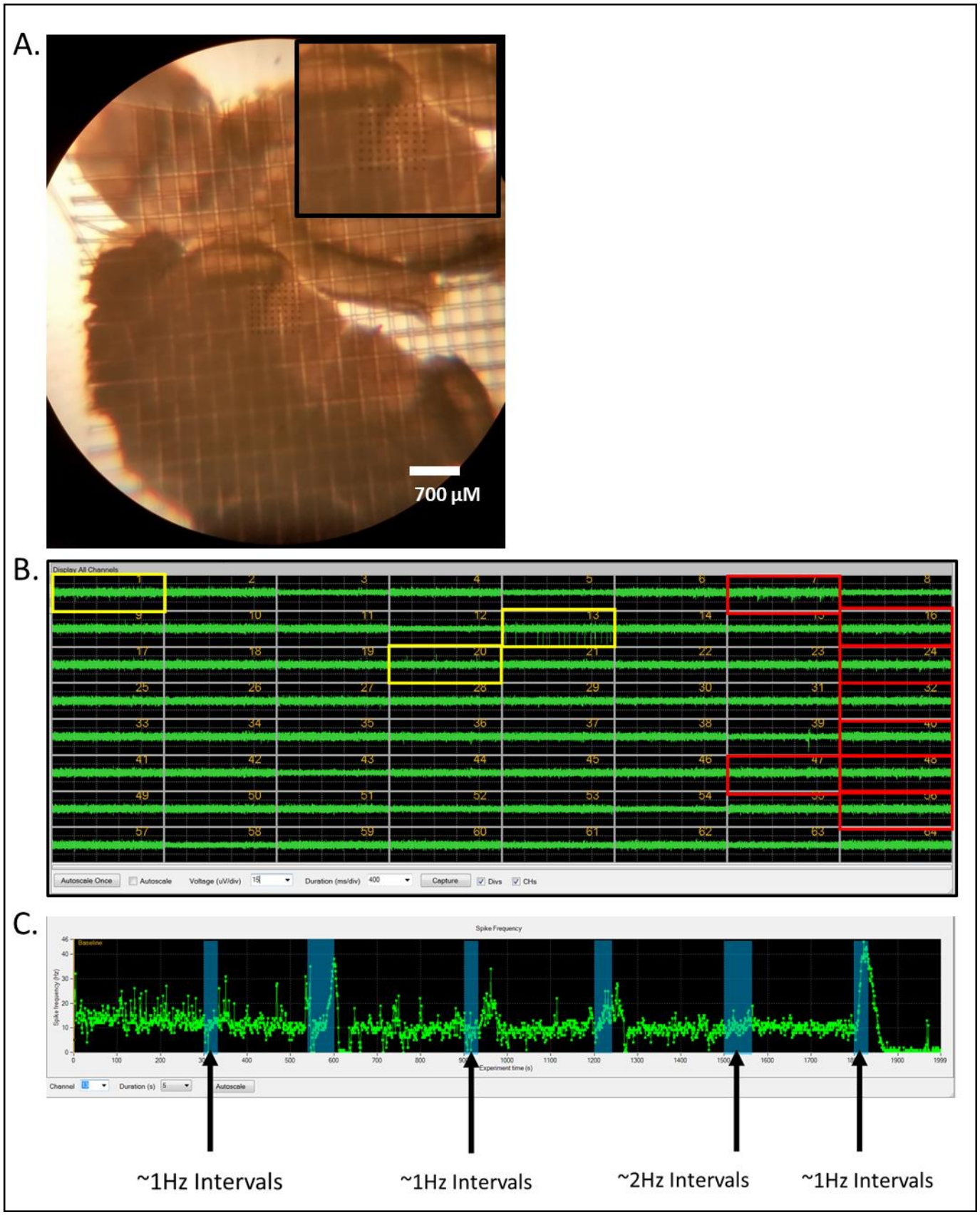
A.
700 µM
B.
Display All Channels
Autoscale Once
Autoscale
Voltage (uV/div)
Duration (ms/div)
Capture
Divs
CHs
C.
Spike Frequency
Baseline
Spike frequency (Hz)
Experiment time (s)
Channel
Duration (s)
Autoscale
~1Hz Intervals
~1Hz Intervals
~2Hz Intervals
~1Hz Intervals

Figure 3. Aquiring Firing Activity from dmLC Neurons with Microelectrode Arrays and Applying Optogenetic Stimulation

A) A photomicrograph showing the location of the microeletrode array positioned on the brain slice at the base of the 4th ventricle. (B) The live recordings taken from the 64 recording electrodes, The optostimulated neurons are highlighted in Red and the inhibited neurons are highlighted in Yellow. The position of these electrodes follows the known locations of the dmLC and LC neurons. (C) Raw spike frequency of Electrode 13, showing constant blue light application and pulses of intermittent light application.

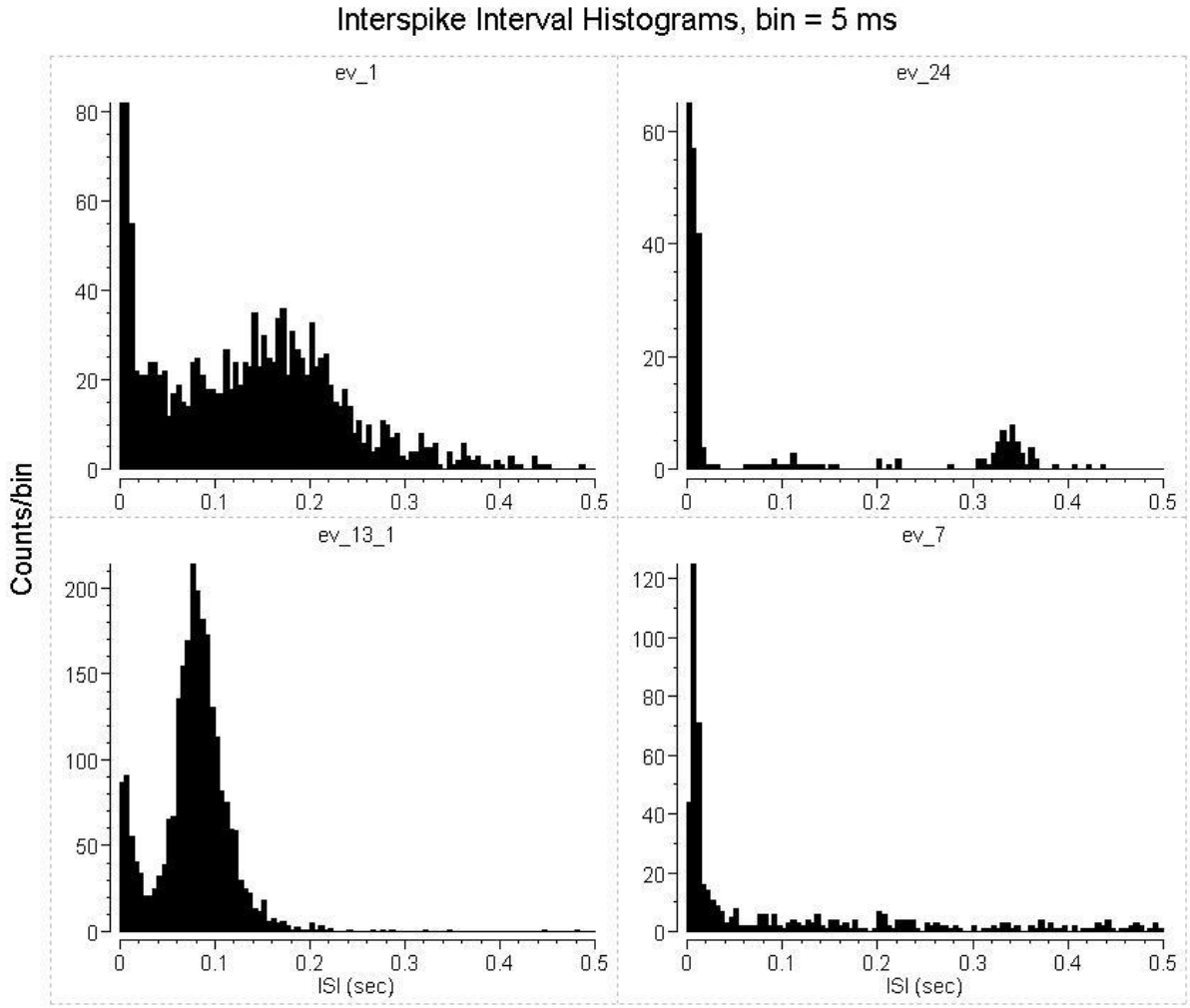

Figure 4. Inter-spike Intervals of Optogenetically Stimulated GABAergic dmLC Neurons and LC Neurons

Inter-spike interval histograms are displayed for 2 optostimulated GABAergic electrodes(ev_24,ev_7) and 2 inhibited LC neurons(ev_1,ev_13_1). The LC neurons show distinctive and constant firing rates that correlate with the values found in patch clamp studies done in our lab. The GABAergic neurons appear to fire almost exclusively during optostimulation and have a very high frequency during this period.

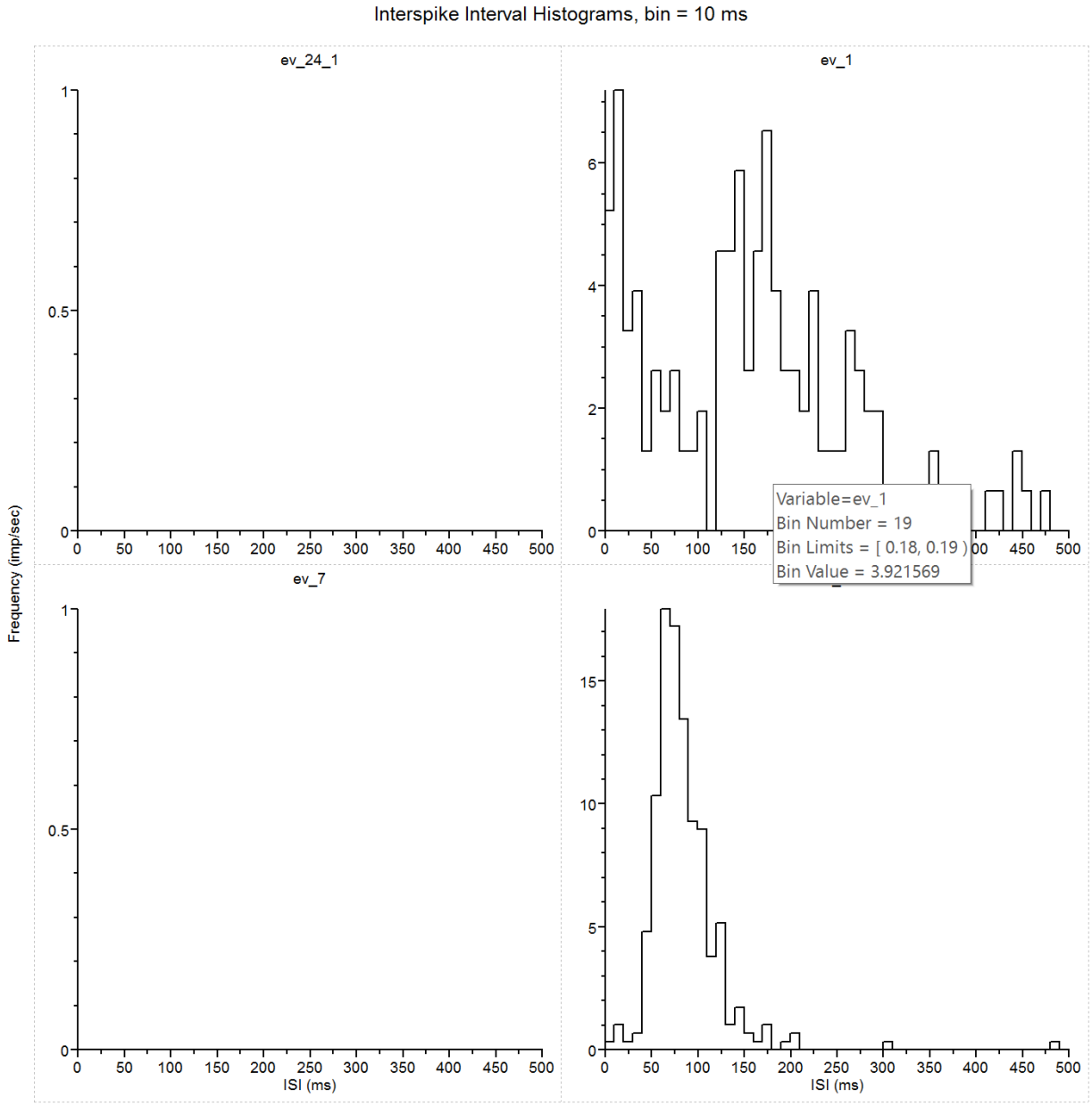
Interspike Interval Histograms, bin = 10 ms
ev_24_1
ev_1
ev_7
Frequency (imp/sec)
ISI (ms)
ISI (ms)
Variable=ev_1
Bin Number = 19
Bin Limits = [0.18, 0.19)
Bin Value = 3.921569

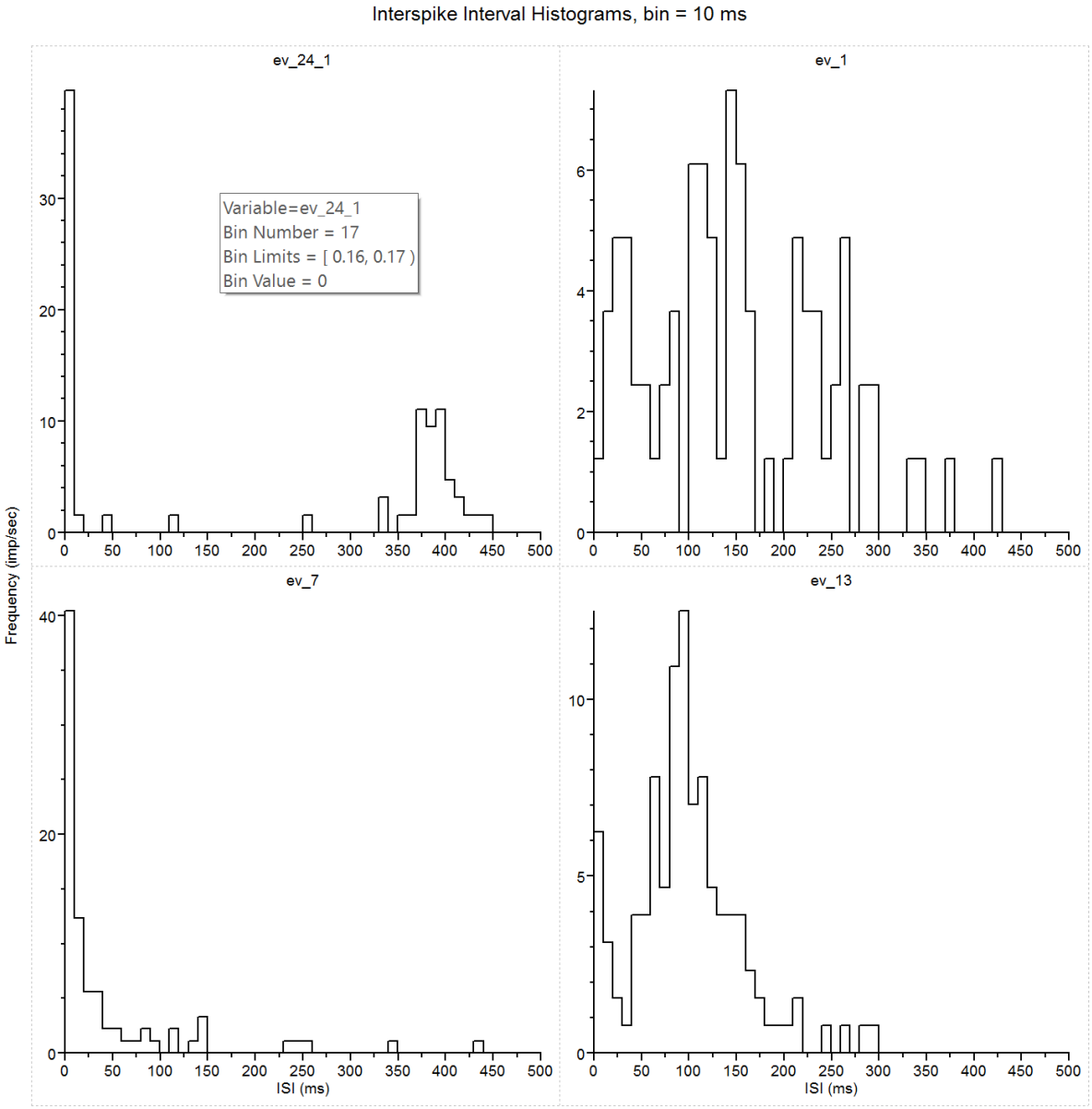

Figure 5. Inter-spike Interval Plots Comparing the Intermittent Optostimulation Response between dmLC and LC Neurons.

Interspike interval histrograms displaying 2 optostimulated GABAergic electrodes(ev_24,ev_7) and 2 inhibited LC neurons(ev_1,ev_13_1). The time period displays 15 seconds before intermittent optostimulation (Top) and 15 seconds during (Bottom) optostimulation at a 1 Hz frequency of 500 ms long pulse. The pre-optostimulation shows the inactivation of the GABAergic neurons and the higher frequency of spiking and lower overall ISI in the LC neurons compared to the post-optostimulation histograms.

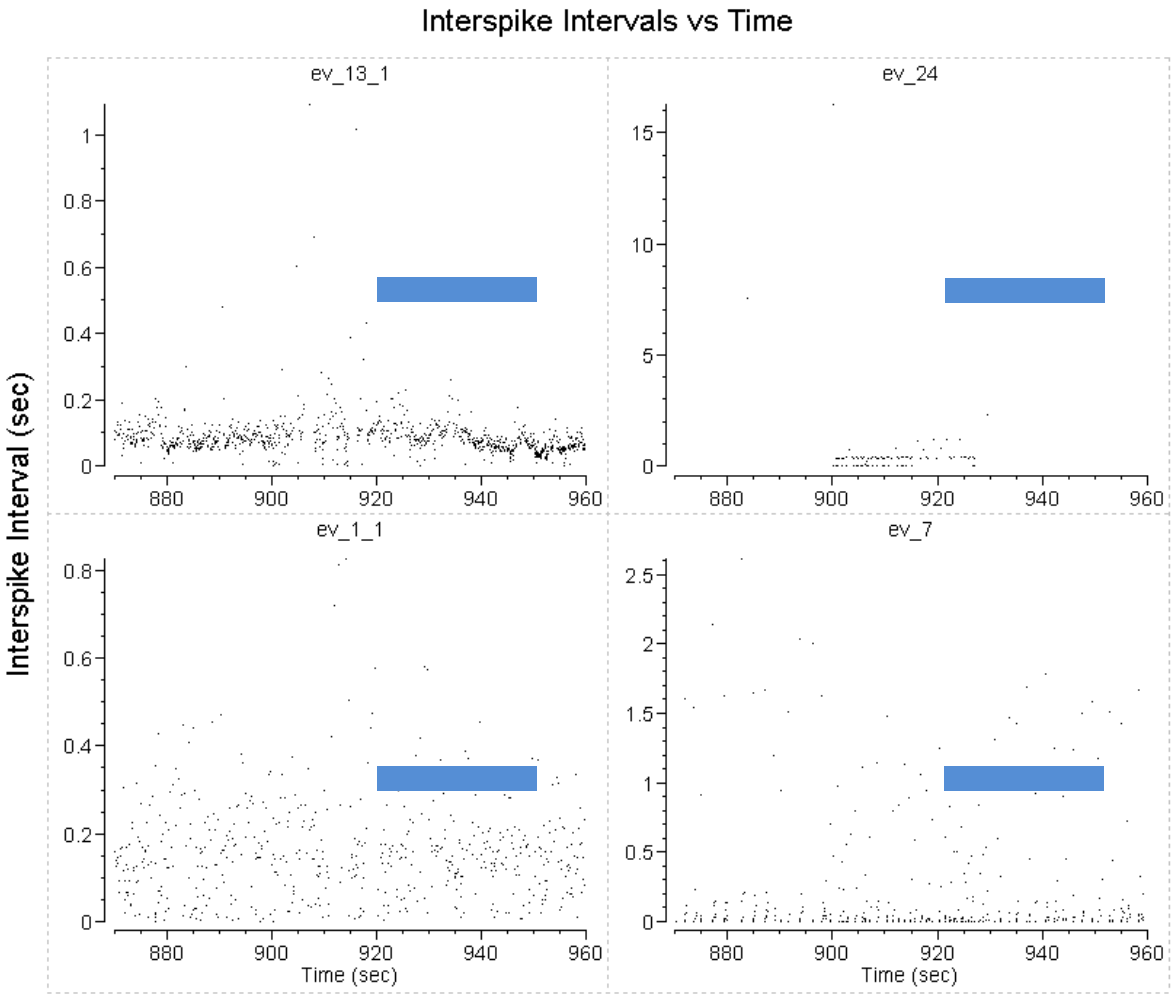

Figure 6. The Inter-spike Interval Response to Optogenetic Light Stimulation Over Time

Inter-spike interval vs time graphs displaying 2 optostimulated GABAergic electrodes(ev_24,ev_7) and 2 inhibited LC neurons(ev_1,ev_13_1). The time period displays 30 seconds before after and during optostimulation at a 1 Hz frequency of 500 ms long pulse. Blue bars indicate during of intermittent, 1 Hz, 500 ms pulse blue light application.

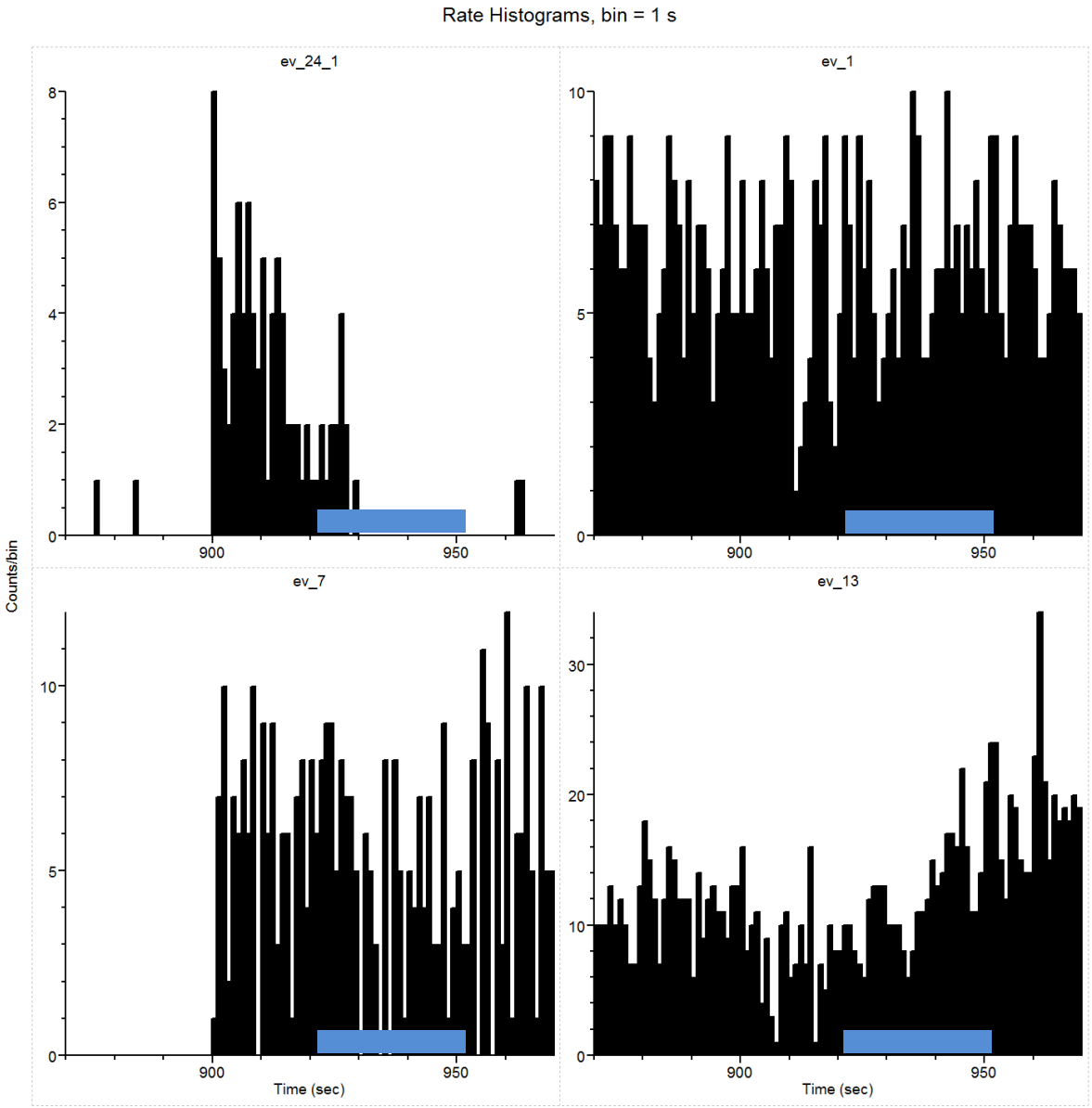

Figure 7. Comparison of Spike Rates Between GABAergic dmLC and LC Neurons
Spike rate histograms are displayed for 2 optostimulated GABAergic electrodes(ev_24,ev_7) and 2 inhibited LC neurons(ev_1,ev_13_1). The time period displays 30 seconds before after and during optostimulation at a 1 Hz frequency of 500 ms long pulse. The optoactivation of the GABAergic neurons is seen in the higher firing rate, while the lower firing rate of the LC neurons demonstrates inhibition. The bar in blue shows the light pulse duration.

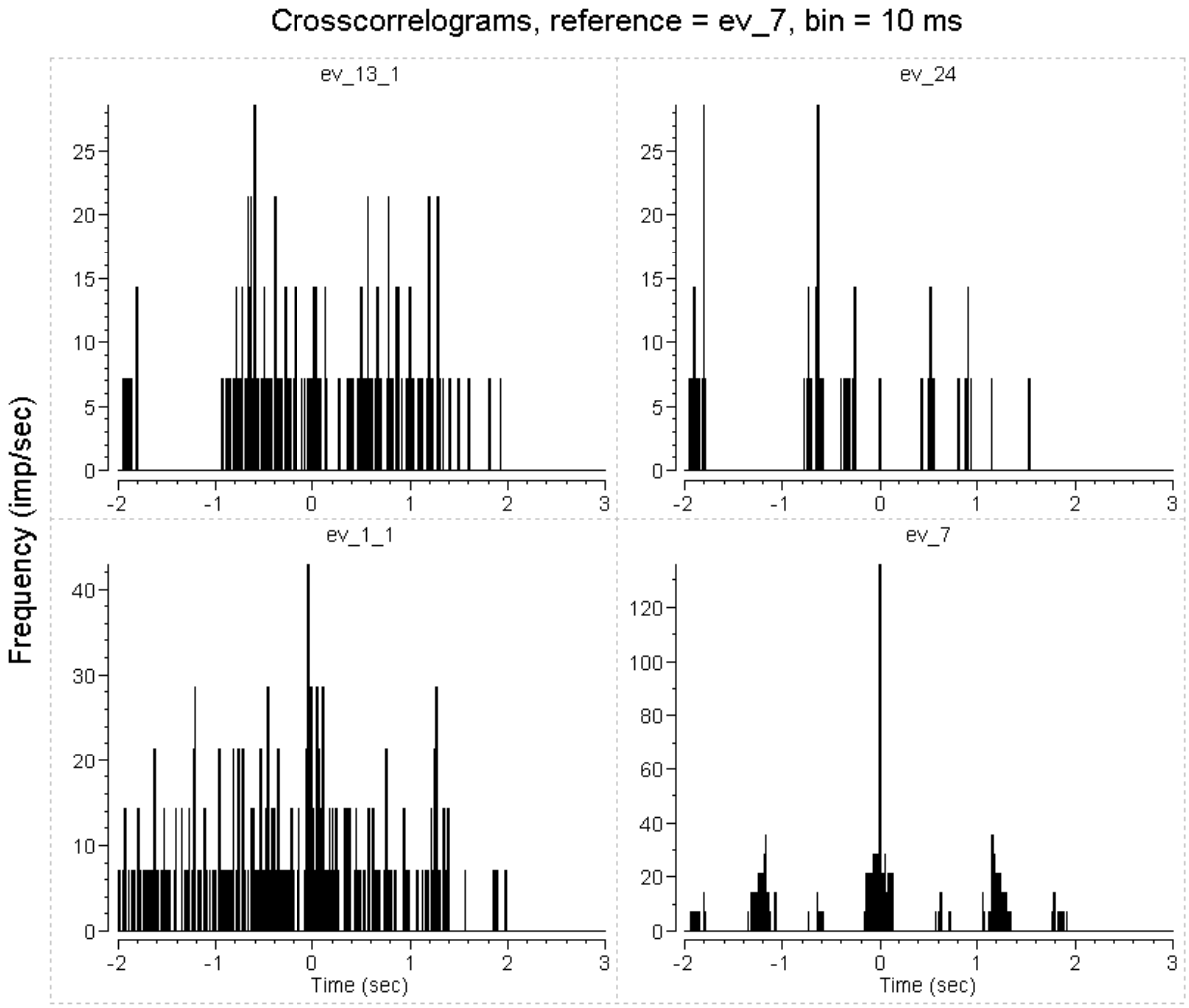

Figure 8. Cross-correlation Between Optostimulation of GABAergic dmLC and LC Neurons

Cross-correlation histograms displayed for 2 optostimulated GABAergic electrodes(ev_24,ev_7) and 2 inhibited LC neurons(ev_1_1,ev_13_1). The analysis references the GABAergic neurons to the LC neurons during a 4 second interval during optostimulation at a 1 Hz frequency with 500 ms long pulses. The inhibition of LC neuron ev_13_1 by GABAergic neuron ev_7 is demonstrated by the significant valley around time 0.

4 INTRODUCTION – SUB AIM 2

4.1 Locus Coeruleus Input to Respiratory Control Areas

Noradrenergic neurons of the locus coeruleus project to the cerebellum, forebrain, spinal cord, and the brainstem, and comprise an estimated ~50% of total noradrenergic projections found in the central nervous system.[36] It has been found that the LC may provide tonic input to the basal respiratory drive, and is associated with chemosensitivity, as it has been identified that focal acidosis of the area stimulates ventilation and ablation causes a reduction in the CO_2 stimulated ventilation.[37], [38] Previous studies have shown that electrical and chemical stimulation introduced to the LC can attenuate the inspiratory inhibition produced by electrical stimulation of the Bötzinger Complex, which suggests that the LC may have a role in the modulation of the inspiratory inhibition of the Bötzinger Complex.[39] The neurons of the LC have also been shown to produce a tonic inhibitory effect on IX respiratory activity in neonatal rat brainstem-spinal cord preparations through the alpha2 adrenergic receptor suggesting that the LC may additionally be involved in regulating the upper-airway expiratory activity.[40]

It has been speculated that projections from the LC to the central pattern generator, or more directly to the respiratory premotoneurons, could be mediated through LC GABAergic neurons.[41],[42] The mitigation of a hypercapnic ventilator response through LC ionotropic receptors could then be attributed to excitatory projections of glycinergic Bötzinger Complex neurons that are associated with the termination of inspiration.[42], [43] The interactions between LC neurons and the glycinergic Bötzinger Complex.is still not clear, so it remains important to investigate how the GABAergic system and disruptions to it can possibly alter breathing regulation associated with these brainstem regions.

4.2 **Rett Syndrome Disrupts Brainstem Respiratory Neuron Pattern Generation**

Individuals who have Rett Syndrome demonstrate irregular breathing that is identified by periodical hypoventilation and compensatory hyperventilation. The RTT-type hypoventilation, including apnea, hypoapnea, and breath hold, is found in both human and animal models, and increases in severity as the disease progresses.[44], [31] The mechanisms under which this hypoventilation occurs remains unclear, but the dysfunction of the brainstem respiratory neuronal activity appears to play a critical role. Hypoventilation may possibly be attributed to insufficient central inspiratory activity, which could lead to a decrease in the inspiratory premotor output.[45], [46] An insufficient amount of activity in the central inspiratory pattern could be associated with a shortened inspiratory burst as well as a decrease of inspiratory spike frequency, in concert with increases in the expiratory activity. Although, there are cellular events that may be at work as well, of which include the reshaping of firing patterns from respiratory neurons, altered grouping, and unpredictable firing activity in some major brainstem respiratory neuronal groups.

Identifying the cellular processes that underlie RTT-type hypoventilation could be useful in producing some novel therapeutic strategies. Therefore, we conducted *in vivo* electrophysiology recordings in the brainstem, targeting respiratory neurons and the phrenic nerve of *Mecp2*-null rats. The *Mecp2*-null rats replicated a RTT model that recreates most of the human RTT phenotypes and enabled *in vivo* experimentation.[31] We use these approaches to investigate and classify inspiratory (I) and expiratory (E) neurons in the brainstem, and associate the firing activity with hypoventilation in *Mecp2*-null rats. By investigating the pattern generation of these respiratory neurons, and applying GABAergic agonists and uptake inhibitors, the effect of GABAergic projections on this pattern generation can be further studied.

5 MATERIALS AND METHODS – SUB AIM 2

5.1 In vivo Electrophysiology

The *in vivo* experiments were conducted using both *Mecp2*-null (*Mecp2*$^{-/Y}$) and wild-type (WT) rats. In general, the electrophysiological experiments were conducted as previously described.[35] The rats were mounted on a stereotaxic setup where a craniotomy, decerebration and partial cerebellum extraction were performed in succession. The phrenic nerve was then isolated for recording field potential activity using a glass-coated tungsten microelectrode. The spikes recorded this way were assorted using an offline sorting tool to classify the spikes by firing rate. Spikes with clear respiratory rhythms were isolated and used for further data analysis.

5.2 Plethysmography

The breathing activity of conscious animals was measured at ages P21-P81 using plethysmography. Whole body plethysmography was conducted on individual rats using a cylindrical ~1100-ml body box to record breathing activity over time. Individual animals were held in the plethysmograph chamber with circulating air running at a rate of ~1000ml/min. Following a 20-minute adaptation, breathing activity was acquired for a further 20 minutes. Data was processed using Clampfit 10.3 software and amplified using AxoScope 10.2 software.

5.3 Drug Administration

During the stereotaxic rat preparation, drugs were injected into the animals as in vivo electrophysiology recordings were conducted. The drugs THIP (tetrahydroisoxazolo (5,4-c)pyridin-3-ol, purchased from Tocris)[1,2] (a GABA agonist, 20mg/kg, i.p.) and NNC-711 (a GABA reuptake blocker, 10mg/kg, i.p.) were used alongside a saline control.

5.4 **Transgenic Animals**

All animal experimentation was produced following the National Institutes of Health (NIH) *Guide for the Care and Use of Laboratory Animals* with approval from the Georgia State University Institutional Animal Care and Use Committee. Experiments were conducted on male *Mecp2*$^{-/Y}$ rats because using a male model allowed for a complete *Mecp2*-null condition that is not generally observed in the female due to variable X-chromosome inactivation.[33],[34] In order to breed these males and genotyping protocol was followed as previously described using a protocol from Sage Labs in Horizon Discovery Group and a 71 bp deletion in the *Mecp2* (Primer F: GCAGCATCAGAAGGTGTTCA, Primer R: GACCTCAATGCTGACGGTTT).[31]

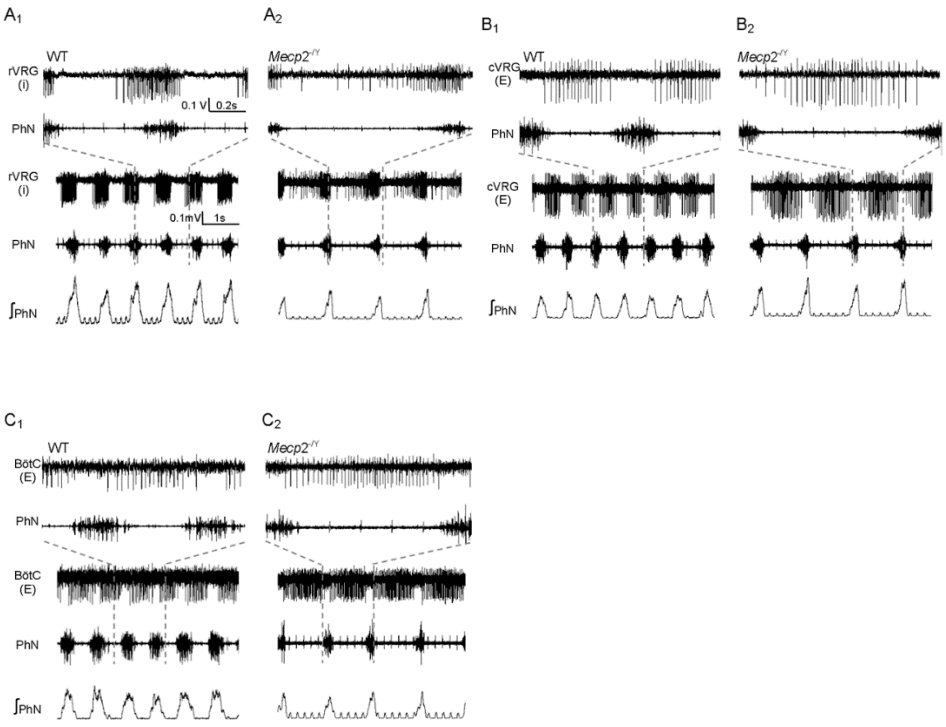

Figure 9. Comparison of Breathing Activity of Wildtype and Mecp2 Knockout Rats, Taken from Multiple Brainstem Regions

Figure 9 Recordings from the in vivo microelectrode are displayed in A, B, and C where neurons from the rostral VRG (rVRG), phrenic nerve (PhN), Bötzinger Complex area (BötC), and caudal VRG (cVRG) were isolated in both the wild-type and Mecp2-/Y rats.Neurons with inspiratory rythem (I) were identified between the rVRG, while expiratory (E) neurons were identified in the cVRG and BötC. Integrated burst activity is displayed in the final trace for the phrenic nerve activity.

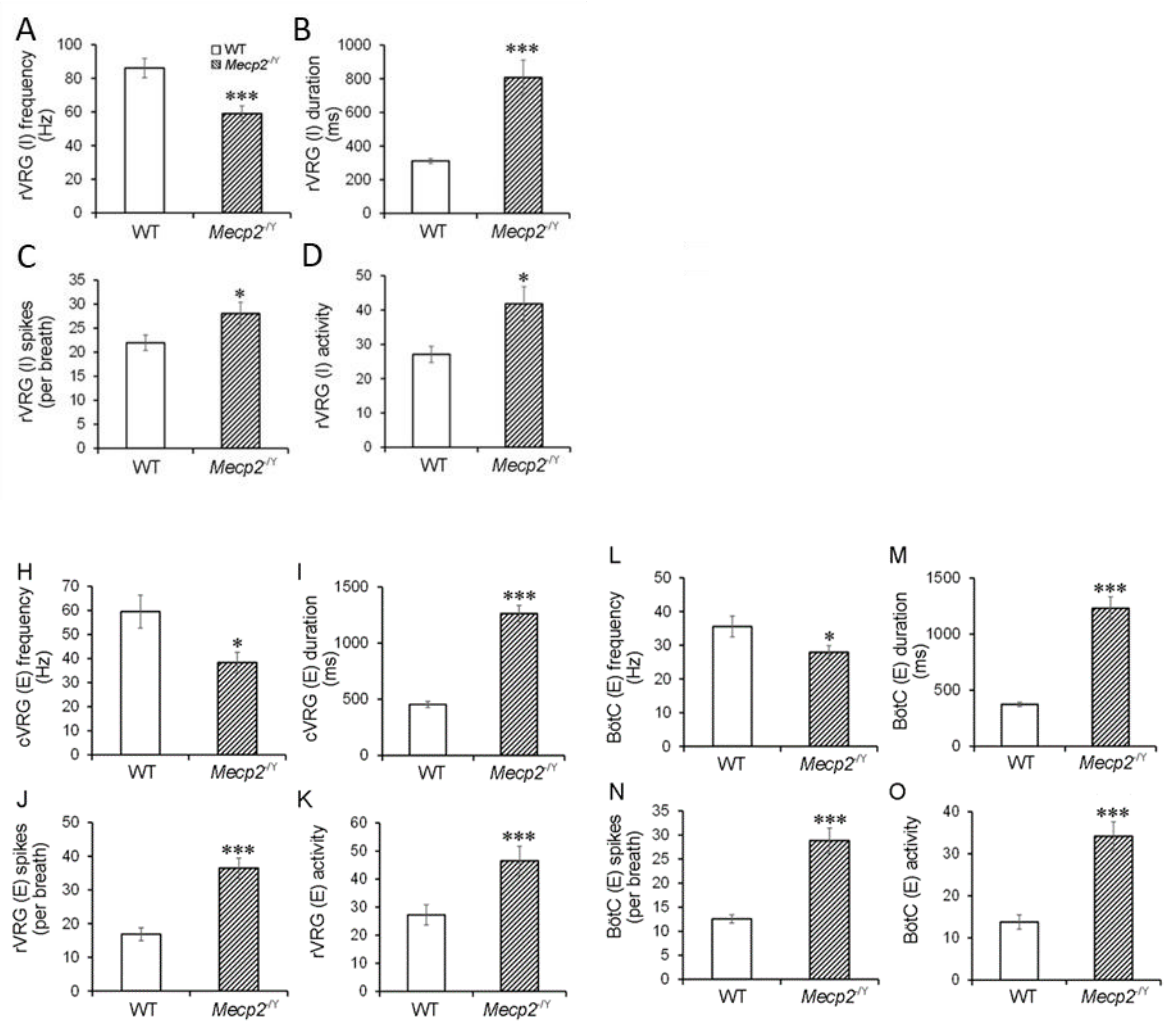

Figure 10. Firing Frequency Compared Between Wildtype and Mecp2 Knockout Rats, Taken from Various Brainstem Regions

*Firing frequencies are shown in A, H, and L for neurons in the rostral VRG (rVRG), caudal VRG (cVRG), Bötzinger Complex area (BötC), and were isolated in both the wild-type and Mecp2$^{-/Y}$ rats. The overall firing rates were lower in the Mecp2 null rats than in the wild-type rats for these three groups of neurons. The burst duration and number of spikes (F,J,N) within each burst was higher in the Mecp2 null rats than in WT rats. When the neuronal activity was compared as a function of frequency x duration (G,K,O), there were significantly higher levels in the WT rats when compared the the Mecp2 null rats. *, P<0.05; **, P<0.01; ***, P<0.001 (Student's t-test).*

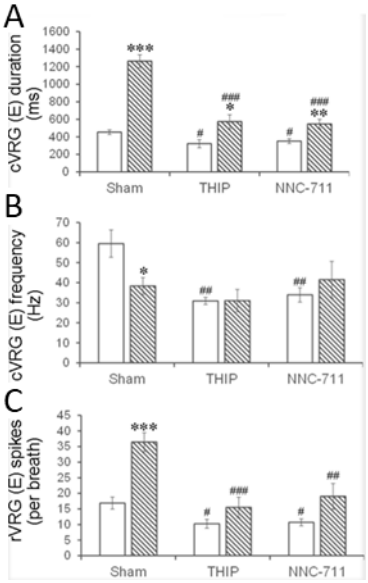

Figure 11. Comparison of THIP and NNC-711 Treatment on Respiratory Neuron Activity Between Wildtype and Mecp2 Knockout

Increased excitation of respiratory neurons during periods of defined apnea, suggested that there were higher levels of excitation over depression in activity in Mecp2 null rats. Identifying this increased excitability as a disease-state phenotype, we chose to intervene in the GABAergic neuronal network. Burst duration, firing frequency and number of spikes per burst are shown following treatment with THIP and NNC-711 (A,B,C). (Two-way ANOVA followed by a Bonferroni post-hoc test shows significant difference comparing the WT to Mecp2$^{-/Y}$, # designates the significant difference between the Sham, THIP, or NNC-711 models between the two genetic rat groups.)*

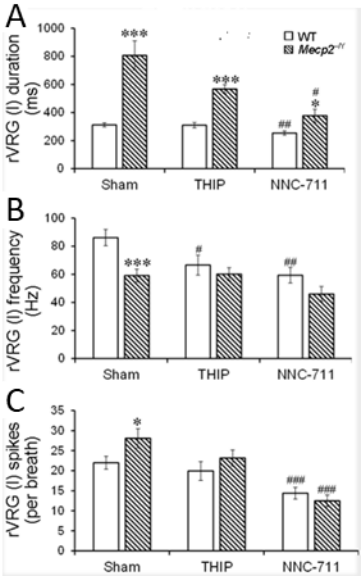

Figure 12. Comparison of THIP and NNC-711 Treatment on Inspiratory Neuron Activity Between Wildtype and Mecp2 Knockout

The inspiratory group of neurons primarily focusing on the rVRG is compared above using burst duration, firing frequency and number of spikes per burst which are shown following treatment with THIP and NNC-711 (A,B,C). (Two-way ANOVA followed by a Bonferroni post-hoc test shows significant difference comparing the WT to Mecp2$^{-/Y}$, # designates the significant difference between the Sham, THIP, or NNC-711 models between the two genetic rat groups.)*

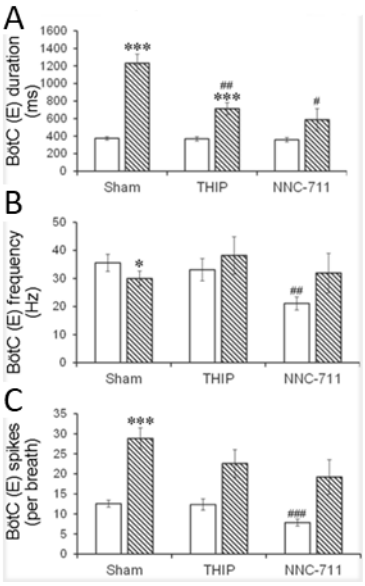

Figure 13. Comparison of THIP and NNC-711 Treatment on BotC Expiratory Neuron Activity Between Wildtype and Mecp2 Knockout

The BotC expiratory group of neurons primarily focusing on the BotC is compared above using burst duration, firing frequency and number of spikes per burst which are shown following treatment with THIP and NNC-711 (C,F,I). (Two-way ANOVA followed by a Bonferroni post-hoc test shows significant difference comparing the WT to Mecp2$^{-/Y}$, # designates the significant difference between the Sham, THIP, or NNC-711 models between the two genetic rat groups.)*

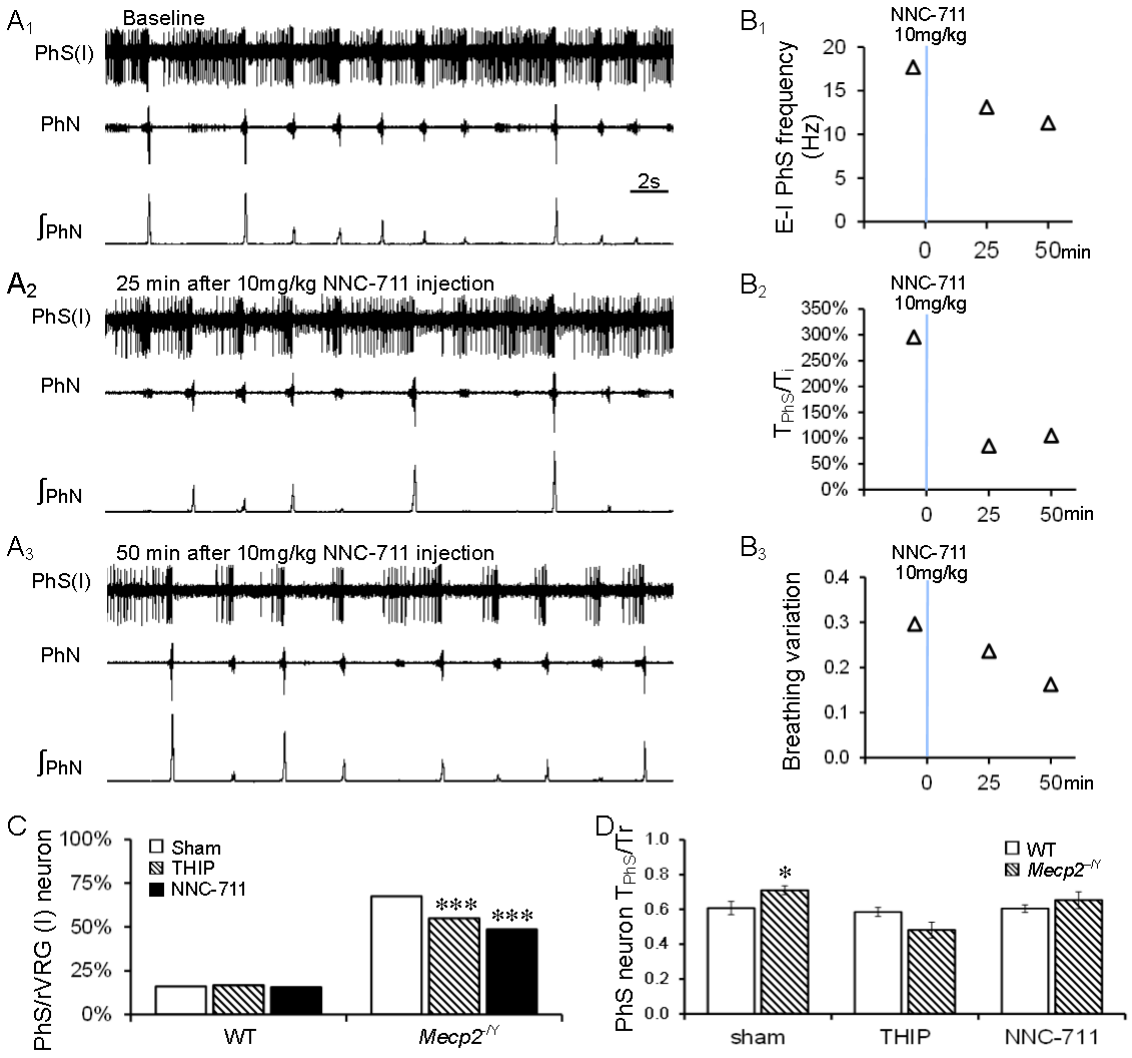

Figure 14. The Effect of NNC-711 and THIP on Phrenic Nerve Activity Over Time and the Breathing Activity Variation Between Wildtype and Mecp2 Knockout.
The traces above (A) show expiratory to inspiratory neurons from the PhN over an hour long recording following administration of the drug NNC-711. There was a decrease in the firing frequency and burst duration of these expiratory and inspiratory neurons and in phrenic breathing variation following treatment with NNC-711 (B). Expiratory and inspiratory neurons when inversely correlated to all the rVRG cells recorded, displayed reductions following treatment with 20mg/kg THIP and 10mg/kg NNC-711 in Mecp2$^{-/Y}$ rats (C). (x^2 test) The differences between burst durations disappeared following GABAergic augmentation when comparing Mecp2-/Y and WT rats (D). (Two-way ANOVA)

6 RESULTS – SUB AIM 2

6.1 *In Vivo* Electrophisology of Respiratory GABAergic Neurons in the Brainstem

The deletion of the gene *Mecp2* produced an increase in the overall firing activity of neurons residing in the ventral respiratory column of the rat population.[31] It was identified that there is a large group of cells in this knockout model that were classified as E-I phase-spanning neurons that demonstrated a significant increase in burst duration. Neurons located in the Bötzinger Complex area and identified as Post-Inspiratory neurons, were found to be located more rostro-dorsally in knockout rats than in wildtype rats. Apneas were observed at a high frequency with the Mecp2 knockout rats, and respiratory neurons continued to remain active despite an abundance of ectopic single-unit phrenic discharges (Fig. 9). When injected into the rats, THIP and NNC-711 drug treatment significantly diminished the differences in the brainstem respiratory firing activity occurring between the knockout and wildtype rats. It appears that the knockout of *Mecp2* in these rats causes an augmentation of firing activity in the medullary respiratory neurons that is significantly reduced when GABA receptor agonists or uptake blockers are introduced.

6.2 Inspiration

The bulbospinal premotor neurons identified as rostral ventral respiratory group (rVRG) neurons, were characterized by their association with inspiratory phase breathing patterns. The inspiratory drive to the spinal phrenic motoneurons is produced by the neurons in the brainstem region, so given the location in the brainstem and plethysmograph phenotype, characterization of these neurons as part of the rVRG is plausible. Inhibition by the expiratory Bötzinger Complex neurons on the neurons of the rVRG prodcues a characteristic ramping pattern in the breathing activity. Firing rates for the Mecp2 knockout rVRG inspiratory neurons went up following THIP

and NNC-711 drug treatment, indicating that more available GABA allowed for the inhibition of expiratory neurons feeding into the rVRG inspiratory pattern generation. As observed in (Figure 13.), the BötC area showed significant reductions in burst duration after the drug treatment.

*6.3 **Expiration***

The expiratory phase was defined by input detected from both the Bötzinger Complex area and caudal ventral respiratory group (cVRG) neurons which receive input from the Bötzinger Complex. The BötC is made up primarily of expiratory neurons, of which glycinergic and GABAergic neurons have been shown to inhibit the inspiratory neurons to create the inspiratory-expiratory phase alternation during normal breathing. Firing activity in Mecp2 knockout rats was observed at a higher frequency, and when injected with THIP or NNC-711, this difference was significantly increased in the BötC, suggesting that GABAergic input through the BötC was affected (Fig. 13). The BötC expiratory neurons form the primary source for inhibition to inspiratory neurons through expiration,[39] so for the burst duration and spike count to increase following GABA inhibitory drug treatment would suggest that GABAergic input to the BötC neurons is being suppressed and that reduction is having a subsequent effect on neurons in the ventral respiratory column.

The cVRG comprises the bulbospinal expiratory neurons in the region of the ventral respiratory group caudal to the rVRG neurons. Neurons in the cVRG receive convergent input from the BötC and the RTN/pFRG, and this produces the expiratory drive to the lumbar and spinal thoracic expiratory motoneurons. Burst durations of cVRG identified breathing activity, was reduced to fall in range of the wildtype rat when THIP and NNC-711 were introduced to the Mecp2 rats (Figure 11), this suggests a reduction in hyperexcitation of cVRG expiratory neurons. The frequency of firing activity fell within range following drug treatment, a >60% difference

between wildtype and knockout rats was normalized to within <1% under THIP treatment. The expiratory input coming from the BötC is inhibitory to the activity of the neurons in the cVRG, so an increase in the expiratory spike number in the BötC can explain a decreased firing activity and burst duration in the expiratory neurons of the cVRG.

6.4 GABA Inhibition

It has been well observed in previous studies that there is a reduction in GABAergic inhibition in the brainstem of *Mecp2*- null mice, leading to increased excitability of medullary respiratory neurons.[19] By augmenting the GABAergic synaptic inhibition, it could be possible to decrease the variation in respiratory neuronal firing. We used this type of rational when applying the drug NNC-711, a GABA uptake transport blocker that should functionally promote accumulation of GABA and increase GABAergic synaptic transmission. Treatment with NNC-711 at 10mg/kg resulted in a decrease in the difference of neuronal firing activity when comparing the null and WT rats. There were even indications that in some rats, the discrepancy was eliminated (Fig 14). The effect was found to be more accentuated on the rVRG and cVRG neurons (Fig 14). In the BötC of null rats, the neuronal activity was only mildly affected by the GABA uptake blocker. The compound THIP, an extra synaptic receptor agonist that was also applied, showed similar results (Fig 14).

A dose of NNC-711 would begin to have an observable effect about 20 minutes following injection. The proportion of phase-spanning neurons in the rVRG decreased in MECP2-null rats from 49% to 59% following treatment with either NNC-711 or THIP, both from around 71%(Fig 14).

7 CONCLUSIONS

Through this study we have used optogenetics and microeletrode arrays to observe the interactions of GABAergic neurons involved in breathing regulation in the brainstem. By expressing ChR2 in GABAergic neurons, we were able to investigate the dorsomedial LC region which is interconnected with the LC neurons in the brainstem. Field potential signals recorded from these neurons displayed evidence to suggest the direct inhibition of LC neurons by these GABAergic neurons. Signals that were representative of GABAergic interneurons of the dmLC were found in proximity (200-300 um) to neurons that were representative of LC neurons in an array of 64 microelectrodes.

The results indicate that inhibition of LC neurons is directly produced by dmLC optostimulation. Monosynaptic inhibition was suggested in previous research done in our lab, but was not conclusively proven.[8],[12] Optoactivation of the GABAergic neurons in the LC region of the brainstem has shown to induce inhibition of LC neurons in direct communication with GABAergic interneurons of the dmLC (Fig .8). The possibility that light is activating axons of GABAergic neurons was left open as a possible alternative to monosynaptic inhibition, directly by the dmLC. However, the interactions between the firing events of GABAergic optostimulated neurons and LC neurons increased the ISI during these periods, and thus would suggest a direct inhibition through a monosynaptic communication is more likely.

The dmLC neurons were identified as GABAergic and form an isolated and densely packed nucleus in close contact to the LC neurons.[8] They were found to inhibit LC neurons through oligosynaptic interactions of the local LC neuronal circuitry. LC neurons display inhibition following the activation of dmLC neurons, but the inhibition is not directly

monosynaptic. The delay in inhibition and the lack of a cross correlation between firing events from the GABAergic neurons and the noradrenergic LC neurons would suggest there are intermediate neurons affecting the circuit. We see a higher latency than previous studies, (>3 ms), which would suggest a polysynaptic interaction over a monosynaptic interaction.[8] There is then more reason to suggest that these GABAergic neurons act as interneurons sending a feed-forward signal from other unknown brain regions.

In the *in vivo* experiments conducted by Yang Wu, it is shown that the disruption of the GABAergic communication in the brainstem is having a direct effect on the breathing pattern in the rat model of Rett Syndrome. After characterizing phrenic nerve activity, (Fig .9), and the increased numbers of apneas associated with the Mecp2 knockout model, GABAergic neurons were treated with a GABA agonist and a GABA reuptake inhibitor and demonstrated the rectification of the apneas and increased firing activity between the wildtype and knockout models (Fig. 10). The subsequent rectification of the disease state following GABAergic modification infers that the breathing pattern is influenced by a lack of inhibition caused by the GABA neurons in the brainstem. The LC propagates its signal pattern generation through the same brainstem regions investigated in the *in vivo* study, the Bötzinger Complex area, and so it can be inferred that this communication is possibly true for the GABAergic input coming from the dmLC GABAergic neurons.

Treatment with the GABA agonist THIP could be influencing brain regions outside the BötC by augmenting the local extra synaptic $GABA_A$ receptor, so LC neurons could be benefiting in the form of an equilibration of excitability. As the LC is the major source for NE in the CNS, any equilibration would promote a stable supply of NE, so hyperexcitability could be a sign that this NE synthesis is impaired in Mecp2 knockout rats.[31],[32] Correction of the

GABAergic input to the LC could be reinstating the homeostatic level in the cells of the ventral respiratory column by improving NE output, projected targets of the LC, such as the brainstem, prefrontal cortex, and spinal cord could all see stabilization.

When looking at the cellular level, the present study reveals evidence for increased excitability of respiratory neurons following Mecp2 disruption. An abundance of excitation in inspiratory cells display phase-spanning patterns that are reversible to the original inspiratory phenotype through enhancement of endogenous GABA inhibition or through GABA receptor agonist THIP. A number of phase-spanning neurons did not transition to inspiratory type, this was most probably due to applying too low of a concentration and too low exposure time of the drug. Expiratory neurons in both the cVRG and the BötC demonstrated increased levels of firing activity. The amount of Post-I cells was significantly diminished in the BötC, a likely result of the increased firing duration combining with other expiratory neurons.

Hyperexcitability is a well-known issue associated with respiratory neurons following Mecp2 disruption.[9],[11],[12] Because there is such a significant effect on the physiological role of breathing, it was necessary to try and apply an acute treatment to intervene immediately. The GABA uptake inhibitor NNC-711 was found to significantly decrease the hyperexcitability found in respiratory neurons when applied, and in further research done by Wu et al., evidence was found for the transformation of a third of neurons from phase-spanning to inspiratory following treatment. We also found evidence to suggest that extra synaptic $GABA_A$ receptor agonist THIP produced similar effects. Wu et al. also recorded that the GABA intervention demonstrated a rescue in breathing phenotypes to a WT state.

The findings, based on both the dmLC investigations in the brainstem, in combination with the evidence produced from the experiments done with Yang Wu, demonstrated that

hyperexcitability in the medullary respiratory neurons was widespread following Mecp2 disruption, which was consistent with a wide range of abnormalities associated with breathing observed in both animal models and people who have RTT.[9],[10],[12],[31] Defective GABAergic systems may be attributable to a large range of breathing related abnormalities in RTT animals.[9],[31] An effective strategy for treating symptoms of RTT in the clinic may well involve intervention of the GABAergic system as it was found here to have a robust effect. Further understanding the interactions of the GABAergic system in the brainstem through *in vitro* and *in vivo* approaches will allow us to pinpoint the targets for these interventions. Successful drug candidates could then be tested in human clinical trials.

REFERENCES

1. Carter, M.E., et al., *Tuning arousal with optogenetic modulation of locus coeruleus neurons.* Nat Neurosci, 2010. **13**(12): p. 1526-33.
2. Chandler, D.J., W.J. Gao, and B.D. Waterhouse, *Heterogeneous organization of the locus coeruleus projections to prefrontal and motor cortices.* Proc Natl Acad Sci U S A, 2014. **111**(18): p. 6816-21.
3. Schwarz, L.A. and L. Luo, *Organization of the locus coeruleus-norepinephrine system.* Curr Biol, 2015. **25**(21): p. R1051-R1056.
4. McCall, J.G., et al., *CRH Engagement of the Locus Coeruleus Noradrenergic System Mediates Stress-Induced Anxiety.* Neuron, 2015. **87**(3): p. 605-20.
5. Schwarz, L.A., et al., *Viral-genetic tracing of the input-output organization of a central noradrenaline circuit.* Nature, 2015. **524**(7563): p. 88-92.
6. Soiza-Reilly, M., et al., *Presynaptic gating of excitation in the dorsal raphe nucleus by GABA.* Proc Natl Acad Sci U S A, 2013. **110**(39): p. 15800-5.
7. Viney, T.J., et al., *Network state-dependent inhibition of identified hippocampal CA3 axo-axonic cells in vivo.* Nat Neurosci, 2013. **16**(12): p. 1802-1811.
8. Jin, X., et al., *Identification of a Group of GABAergic Neurons in the Dorsomedial Area of the Locus Coeruleus.* PLoS One, 2016. **11**(1): p. e0146470.
9. Guy, J., et al., *A mouse Mecp2-null mutation causes neurological symptoms that mimic Rett syndrome.* Nat Genet, 2001. **27**(3): p. 322-6.
10. Zhong, W., et al., *Effects of early-life exposure to THIP on phenotype development in a mouse model of Rett syndrome.* J Neurodev Disord, 2016. **8**: p. 37.
11. Oginsky, M.F., et al., *Hyperexcitability of Mesencephalic Trigeminal Neurons and Reorganization of Ion Channel Expression in a Rett Syndrome Model.* J Cell Physiol, 2017. **232**(5): p. 1151-1164.
12. Jin, X., et al., *GABAergic synaptic inputs of locus coeruleus neurons in wild-type and Mecp2-null mice.* Am J Physiol Cell Physiol, 2013. **304**(9): p. C844-57.
13. Swanson, L.W., *The locus coeruleus: a cytoarchitectonic, Golgi and immunohistochemical study in the albino rat.* Brain Res, 1976. **110**(1): p. 39-56.
14. Klimek, V., et al., *Reduced levels of norepinephrine transporters in the locus coeruleus in major depression.* J Neurosci, 1997. **17**(21): p. 8451-8.
15. Foote, S.L., F.E. Bloom, and G. Aston-Jones, *Nucleus locus ceruleus: new evidence of anatomical and physiological specificity.* Physiol Rev, 1983. **63**(3): p. 844-914.
16. Loughlin, S.E., S.L. Foote, and J.H. Fallon, *Locus coeruleus projections to cortex: topography, morphology and collateralization.* Brain Res Bull, 1982. **9**(1-6): p. 287-94.
17. Biancardi, V., et al., *Locus coeruleus noradrenergic neurons and CO2 drive to breathing.* Pflugers Arch, 2008. **455**(6): p. 1119-28.
18. Jin, X., W. Zhong, and C. Jiang, *Time-dependent modulation of GABA(A)-ergic synaptic transmission by allopregnanolone in locus coeruleus neurons of Mecp2-null mice.* Am J Physiol Cell Physiol, 2013. **305**(11): p. C1151-60.
19. Chao, H.T., et al., *Dysfunction in GABA signalling mediates autism-like stereotypies and Rett syndrome phenotypes.* Nature, 2010. **468**(7321): p. 263-9.

20. Oka, H., et al., *A new planar multielectrode array for extracellular recording: application to hippocampal acute slice.* J Neurosci Methods, 1999. **93**(1): p. 61-7.
21. Shimono, K., et al., *Origins and distribution of cholinergically induced beta rhythms in hippocampal slices.* J Neurosci, 2000. **20**(22): p. 8462-73.
22. Shimono, K., et al., *Chronic multichannel recordings from organotypic hippocampal slice cultures: protection from excitotoxic effects of NMDA by non-competitive NMDA antagonists.* J Neurosci Methods, 2002. **120**(2): p. 193-202.
23. Morin, F.O., Y. Takamura, and E. Tamiya, *Investigating neuronal activity with planar microelectrode arrays: achievements and new perspectives.* J Biosci Bioeng, 2005. **100**(2): p. 131-43.
24. Hofmann, F. and H. Bading, *Long term recordings with microelectrode arrays: studies of transcription-dependent neuronal plasticity and axonal regeneration.* J Physiol Paris, 2006. **99**(2-3): p. 125-32.
25. Honma, S., et al., *Circadian rhythms of arginine vasopressin and vasoactive intestinal polypeptide do not depend on cytoarchitecture of dispersed cell culture of rat suprachiasmatic nucleus.* Neuroscience, 1998. **86**(3): p. 967-76.
26. Krause, M. and Y. Jia, *Serotonergic modulation of carbachol-induced rhythmic activity in hippocampal slices.* Neuropharmacology, 2005. **48**(3): p. 381-90.
27. Calfa, G., et al., *Excitation/inhibition imbalance and impaired synaptic inhibition in hippocampal area CA3 of Mecp2 knockout mice.* Hippocampus, 2015. **25**(2): p. 159-68.
28. Dahlstrom, A. and K. Fuxe, *Localization of monoamines in the lower brain stem.* Experientia, 1964. **20**(7): p. 398-9.
29. Jin, X.T., et al., *Pre- and postsynaptic modulations of hypoglossal motoneurons by alpha-adrenoceptor activation in wild-type and Mecp2(-/Y) mice.* Am J Physiol Cell Physiol, 2013. **305**(10): p. C1080-90.
30. Pimashkin, A., et al., *Spiking signatures of spontaneous activity bursts in hippocampal cultures.* Front Comput Neurosci, 2011. **5**: p. 46.
31. Wu, Y., et al., *Characterization of Rett Syndrome-like phenotypes in Mecp2-knockout rats.* J Neurodev Disord, 2016. **8**: p. 23.
32. Zhong, W., et al., *Effects of early-life exposure to THIP on brainstem neuronal excitability in the Mecp2-null mouse model of Rett syndrome before and after drug withdrawal.* Physiol Rep, 2017. **5**(2).
33. Weaving, L.S., et al, *Effects of MECP2 mutation type, location and X-inactivation in modulating Rett syndrome phenotype.* Am J Med Genet A. 2003 Apr 15; **118**A(2):103-14.
34. Young J.I. and Zoghbi H.Y., *X-chromosome inactivation patterns are unbalanced and affect the phenotypic outcome in a mouse model of rett syndrome.* Am J Hum Genet. 2004 Mar; **74**(3):511-20.
35. Zhang X., et al, *Intrinsic membrane properties of locus coeruleus neurons in Mecp2-null mice.* Am J Physiol Cell Physiol. 2010 Mar; **298(**3):C635-46.
36. Aston-Jones G, Shipley MT, Grzanna R. *The locus coeruleus, A5 and A7 noradrenergic cell groups.* In: Paxinos G, editor. The Rat Nervous System. Academic Press; San Diego, CA: 1995. pp. 183–213.
37. Pineda J, and Aghajanian GK. *Carbon dioxide regulates the tonic activity of locus coeruleus neurons by modulating a proton- and polyamine-sensitive inward rectifier potassium current*. Neuroscience. 1997 Apr; **77**(3):723-43.

38. Filosa, J. A., Dean, J. B., and Putnam, R. W., *Role of intracellular and extracellular pH in the chemosensitive response of rat Locus coeruleus neurones*. J. Physiol. **541**(Pt 2), 493–509. doi: 10.1113/jphysiol.2001.014142.
39. Wang G., et al., *Modulation of inspiratory inhibition of the Bötzinger complex by raphe pallidus and locus coeruleus in rabbits.* Adv Exp Med Biol. 2004; **551**():127-33.
40. Yamanishi T., et al., *Possible involvement of neurons in locus coeruleus in inhibitory effect on glossopharyngeal expiratory activity in a neonatal rat brainstem-spinal cord preparation in vitro*. Neurosci Res. 2008 Jan; **60**(1):2-9.
41. Champagnat, J., et al., *Involvement of amino acids in periodic inhibitions of bulbar respiratory neurones.* Brain Res. **237**, 351–365. doi: 10.1016/0006-8993(82)90447-4
42. Bonham, A. C. (1995). *Neurotransmitters in the CNS control of breathing. Respir.* Physiol. **101**, 219–230. doi: 10.1016/0034-5687(95)00045-F
43. Schreihofer, A. M., Stornetta, R. L., and Guyenet, P. G. (1999). *Evidence for glycinergic respiratory neurons: Botzinger neurons express mRNA for glycinergic transporter 2.* J. Comp. Neurol. **407**, 583–597. doi: 10.1002/(SICI)1096-9861(19990517)407:4<583::AID-CNE8>3.0.CO;2-E
44. Weese-Mayer D.E., Lieske S.P., Boothby C.M., Kenny A.S., Bennett H.L., Silvestri J.M., Ramirez JM, *Autonomic nervous system dysregulation: breathing and heart rate perturbation during wakefulness in young girls with Rett syndrome*, Pediatr Res, **60** (2006) 443–449.
45. Brouillette RT, Hunt CE, Gallemore GE, Respiratory dysrhythmia. *A new cause of central alveolar hypoventilation*, Am Rev Respir Dis, **134** (1986) 609–611.
46. Eckert D.J., Jordan A.S., Merchia P., Malhotra A., Central sleep apnea: Pathophysiology and treatment, Chest, 131 (2007) 595–607.
47. Wu Y., Cui N., Xing H., et al. *Mecp2 Disruption in Rats Causes Reshaping in Firing Activity and Patterns of Brainstem Respiratory Neurons.* Neuroscience. 2019;**397**:107–115. doi:10.1016/j.neuroscience.2018.11.011